Resources, Conservation & Recycling 133 (2018) 331–342

Contents lists available at ScienceDirect

Resources, Conservation & Recycling

journal homepage: www.elsevier.com/locate/resconrec

Toward supplying food, energy, and water demand: Integrated solar desalination process synthesis with power and hydrogen coproduction

Emre Gençer[a,b], Rakesh Agrawal[a,*]

[a] School of Chemical Engineering, Purdue University, West Lafayette, IN 47906, United States
[b] MIT Energy Initiative, Massachusetts Institute of Technology, Cambridge, MA 02139, United States

ARTICLE INFO

Keywords:
Solar energy
Desalination
Coproduction
Hydrogen production
Conceptual process design

ABSTRACT

The increase in population coupled with rising per capita income and associated change in consumption habits will put unprecedented stress on food, energy and water (FEW) resources. Sustainable and reliable fresh water supply is central for life and also for all sectors that support our existence. Uncertainty on water security prompted interest in investigation of renewable energy driven desalination processes. One particularly promising option is to produce fresh water from the two most abundant resources on earth: solar energy and seawater. In this study, using Solar Electricity, Water, Food and Chemical (SEWFAC) process synthesis concept, we explore and identify synergistic integration alternatives of multi stage flash desalination, solar thermal power, and hydrogen production processes. The promising options have been analyzed by detailed process simulation and optimization using an integrated Aspen Plus and MATLAB modeling environment. The proposed process designs can meet the water and electricity demand with rather high conversion efficiencies. Furthermore, integration of solar hydrogen production and hydrogen-fired power plant can enable continuous production of fresh water and electricity in solar-rich water-poor regions. In addition to other metrics, we have evaluated the performance of the desalination process from power point of view with a new metric, Electricity Equivalent Water (EEW) to demonstrate the marginal energy penalty of desalination. Integration of thermal desalination processes with electricity and hydrogen production is a synergistic alliance and can play a pivotal role in approaching FEW nexus.

1. Introduction

Population growth coupled with rising per capita income and shift toward resource intensive consumption habits create unprecedented stress on food, energy and water (FEW) resources. The grand challenge is to develop and implement solutions to sustainably meet humanity's increasing FEW needs with scarcer resources (Gençer et al., 2017). To put into perspective, the current annual global food consumption is 29.6 EJ (converted to equivalent energy number for comparison) (Alexandratos and Bruinsma, 2012), primary energy consumption is 556 EJ (BP, 2017), and water consumption is more than 9 trillion m^3 (Hoekstra and Mekonnen, 2012). The projected increase in FEW demand by mid-century are 70% (FAO, 2015), 50% (EIA, 2015; IPCC, 2014), and 55% (FAO, 2011), respectively.

Given the scale of the challenge, the solution will include a mix of options such as efficient and low CO_2 emission fossil fuel processing (Ramapriya et al., 2014; Tock and Maréchal, 2015), biofuel production from hybrid conversion processes (Mallapragada et al., 2014; Gençer et al., 2014b), waste management and conversion (Hernández and Martín, 2017; Garcia and You, 2017), utility scale energy storage (Gençer and Agrawal, 2016). Solar energy conversion pathways are particularly attractive due to the tremendous potential of solar energy hitting the earth surface. Of course, intermittency, variations in availability and being dilute in nature are challenges to be addressed (Agrawal and Mallapragada, 2010; Gençer et al., 2014a). Our objective is to optimize the utilization of solar energy through process synthesis and integration to supply FEW needs. We adopt the Solar Electricity, Water, Food and Chemical (SEWFAC) concept, which entails systematic synthesis of energy efficient, synergistic processes for optimal utilization of resources (Gençer and Agrawal, 2017a). The FEW production processes are connected by hydrogen, electricity, and fresh water. SEWFAC approach utilizes these connecting elements to complement individual processes by synergistic integration.

In this study, we explore integrated fresh water production processes. Fresh water is an essential, ever-growing need to sustain life on earth. Moreover, water has an indispensable role for numerous sectors

* Corresponding author.
E-mail addresses: emregencer@mit.edu (E. Gençer), agrawalr@purdue.edu (R. Agrawal).
URL: http://www.agrawalrakesh.org (R. Agrawal).

https://doi.org/10.1016/j.resconrec.2018.01.030
Received 12 October 2017; Received in revised form 25 January 2018; Accepted 27 January 2018
Available online 15 February 2018
0921-3449/

such as agriculture, industry and energy. Global agriculture accounts for 75–86% of humanity's consumptive water use (Field and Michalak, 2015; Molden, 2007). Moreover, energy sector uses great quantities of water for hydropower, thermal electric plants, biofuel production, and oil and gas extraction via fracking (Maupin et al., 2014; Larsen et al., 2016). Currently, surface and underground fresh water resources supply the majority of global water demand (Vorosmarty et al., 2000). The availability and consumption trends significantly vary depending on socio-economic state and geographical location of a region (Lam et al., 2016; Carlton et al., 2016). Water resources are becoming scarcer in many geographical locations (Wallis et al., 2014; Liu et al., 2017). This has raised questions on access to water (The Water Project, 2017) and various aspects of water security such as environmental footprint of man-made water management systems (Palmer et al., 2015). Although access to fresh water is an emerging issue for many countries, it has already been a great problem for arid areas of the world such as Middle East and North Africa (MENA) region (Jemmali and Sullivan, 2014). These countries have been relying on production of fresh water form the seawater and brackish water resources using various desalination technologies for decades (MENA, 2011). In 2015, there were almost 20,000 desalination facilities worldwide with total daily fresh water production capacity of about 85 Mm^3 (Voutchkov, 2016).

2. Background on desalination and process integration

Based on the form of the energy used, we can classify current desalination technologies in two categories: (i) Thermal energy driven desalination processes that include Multi Effect Humidification (MEH), Multi Effect Distillation (MED), Multi Stage Flash (MSF), and Membrane Distillation (MD), and (ii) Electricity-driven processes, which is composed of Mechanical Vapor Compression (MVC), Thermal Vapor Compression (TVC), Reverse Osmosis (RO) and Electro Dialysis (ED). RO has the largest share among the installed desalination plants. RO and ED are the two mainly electricity-driven desalination techniques. Both can be used for brackish water (BW) that has a typical salinity level of 0.05–3%. The energy consumption of ED for BW is 3–4 kWh/m^3 while RO requires 0.5–1.5 kWh/m^3. RO process is also used to desalinate seawater, which has a typical salinity level of 3–5%, by consuming 4–10 kWh/m^3 of electricity (Kucera, 2014). Electricity-driven processes work solely with electricity where as heat-driven processes need energy in the form of electricity for driving pumps. For heat driven desalination processes the feed water quality does not change the energy demand dramatically. Thermal processes needs 60–200 kWh/m^3 heat and up to 2–5 kWh/m^3 electricity depending on the process (Kucera, 2014).

Although currently installed desalination capacity is primarily powered by fossil-based energy sources, there is a growing interest in the development of renewable desalination processes. Solar energy amongst other renewable energy sources has a particular advantage with the ability to directly supply thermal energy for heat-driven desalination technologies. However, depending on the temperature level requirement of the process, solar concentrators may be needed.

2.1. Process integration

Process systems engineering tools and techniques are widely used for synthesis and integration of chemical processes to produce fuels, chemicals, and electricity from a combination of resources. This is achieved by developing frameworks for heat integration (Duran and Grossmann, 1986; El-Halwagi, 2006), mass integration (Shenvi et al., 2013; El-Halwagi and Manousiouthakis, 1989), integration of various feedstocks (Floudas et al., 2012; Agrawal and Singh, 2010), and supply chain integration (Guerra et al., 2016). Some of the measures used to evaluate improvements in the performance of integrations include energy efficiency (Hamed, 2005), exergy efficiency (Favrat and Marechal, 2015; Al-musleh et al., 2014), technology selection (Palenzuela et al., 2015). Single or multiple of these objectives are applied to the problem of interest using process simulation tools, equation oriented modeling techniques, and/or a combination of both and solved/optimized.

2.2. Desalination for solar-rich water-poor regions

Considering most of the arid areas have high insolation, utilization of solar energy for desalination has drawn attention in the literature (Li et al., 2013; Shatat et al., 2013). Different desalination techniques, solar collector design and steam generation methods have been examined to investigate solar desalination alternatives (Kalogirou, 1998). Qiblawey and Banat reported an overview of solar thermal desalination processes (Qiblawey and Banat, 2008). It has been also reported that among the desalination techniques humidification–dehumdification, MD desalination techniques are attractive alternatives for renewable energy integration (Mathioulakis et al., 2007; Gonzlez-Bravo et al., 2015). Gude et al. reviewed different renewable energy alternatives and desalination techniques including hybridization of different desalination processes (Gude et al., 2010). Bacha et al. modeled different configurations of thermal storage for continuous operation of solar desalination (Ben Bacha et al., 2007). Various energy recovery configurations for solar Rankine cycle RO desalination plant was studied with identified potential to significantly reduce the cost of the recovery system (Ben Bacha et al., 2007). A low temperature, low pressure desalination system has been proposed that can be operated by waste or solar heat (Chang et al., 2012). A multi objective MINLP that considers the simultaneous minimization of cost and environmental impact of a solar Rankine cycles coupled with RO desalination plant has been developed (Salcedo et al., 2012).

Integration of desalination technology with Concentrated Solar Power (CSP) for simultaneous power and fresh water production is an attractive route to meet energy and fresh water demand. This concept has been proposed in a number of publications with detailed configurations presented in Gonzlez-Bravo et al. (2017), Moser et al. (2010) and Palenzuela et al. (2011a). Gonzlez-Bravo et al. present an optimization approach for designing water desalination systems involving heat integration and waste heat recovery to reduce the desalination cost, energy consumption, and overall greenhouse gas emissions (Gonzlez-Bravo et al., 2017). Moser et al. analyzed possible integration schemes for simultaneous power and fresh water production from solar energy. Two types of solar fields (parabolic trough and linear Fresnel reflector) and two types of desalination technologies (MED and RO) have been included in the study with thermal storage and fossil fuel added as backup energy sources (Moser et al., 2010). Palenzuela et al. presented a detailed study for production of 50 MWe net power and ~49 km^3/day fresh water with four different configurations. These configurations include various combinations of RO, low temperature (LT)-MED, Thermal Vapour Compression (TVC), and Parabolic Trough (PT)-CSP (Palenzuela et al., 2011a). Desalination integrated with CSP has been discussed in detail in this study and alternatives have been evaluated for Middle East and North Africa (MENA) region (Palenzuela et al., 2011a). A techno-economic feasibility analysis was performed by the Cyprus Institute for Concentrating Solar Power and Desalinated Water (CSP-DSW) Project in 2010. The study proposed to use CSP on Demand (CSPonD) technology, which is a combined solar collection and thermal storage technology (Slocum et al., 2011).

In addition to the above studies, various cogeneration solutions have been proposed by integrating desalination technologies such as multi stage flash or Multi Effect Distillation with the traditional steam cycles or gas turbines (Palenzuela et al., 2011b; Wang and Lior, 2007a,b). However, to the best of our knowledge, a thorough study of solar power integration has not been previously reported on the process level. The overall solar energy conversion efficiency can be increased by judiciously integrating processes that have complementary attributes. Here, we present integrated solar thermal process designs for (i) efficient fresh water and electricity production, and (ii) fresh water,

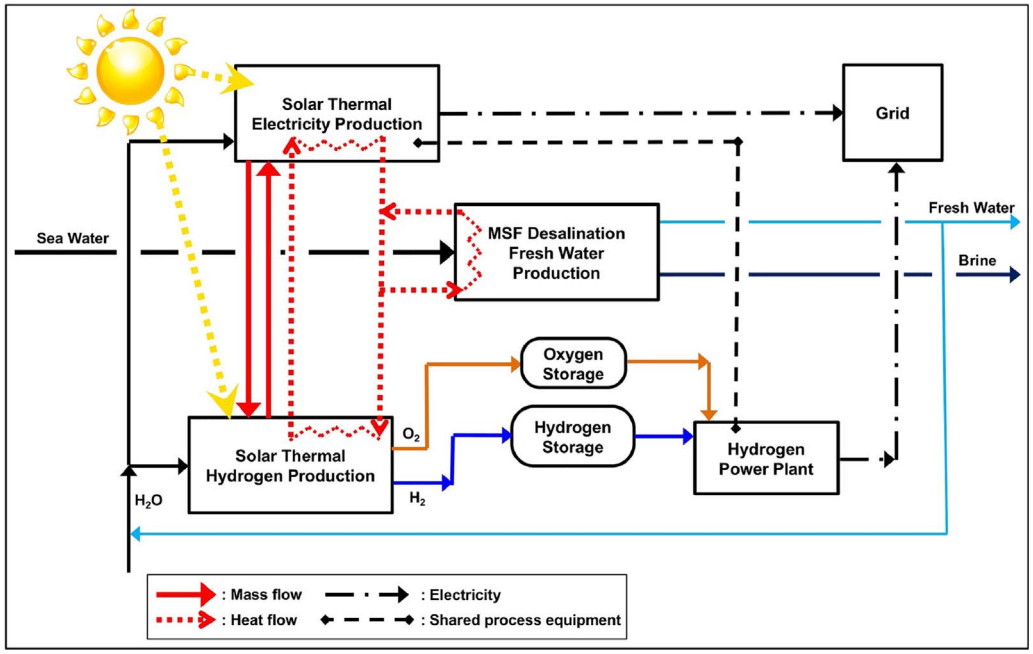

Fig. 1. Process design strategy for triproduction process by allowing heat and mass transfer between solar thermal hydrogen production, solar thermal electricity generation and thermal MSF desalination processes.

electricity, and hydrogen production.

3. SEWFAC for desalination

Integrating thermal desalination processes with solar thermal electricity and hydrogen processes is promising due to the common process units and potential heat and mass integration alternatives. The strategy to design triproduction processes with synergistic integration is shown in Fig. 1. We have identified some of the potential integrations between these processes that are depicted in Fig. 2, where solar thermal power and hydrogen production sections are demonstrated in Fig. 2(a) and multi stage flash desalination related process steps are shown in Fig. 2(b). Circles with plus sign represent streams that need to be heated, circles with minus sign represent streams that need to be cooled down, and diamond signs represent potential common streams for which the entire or a portion of the stream can be transferred between two processes, i.e. the intersection points of the processes. Potential common streams are selected based on similar properties (temperature, pressure, salinity, etc.) of the streams. It should be noted that theses streams do not necessarily have identical properties for their base cases but they can be adjusted by minor modifications in the processes. For illustration of possible integrations, among many options four particular integration schemes marked by numbers (1–4) in Fig. 2 will now be discussed. Feed water is essential for hydrogen production, as marked by 1, a portion of the fresh water produced from desalination plant can be fed to the solar thermal power and hydrogen coproduction plant. In this example, the water is fed at ambient pressure to use fewer high pressure pumps in the overall process. The second integration marked by 2 in Fig. 2 is to transfer fresh water from the discharge of the heat recovery stages of the desalination plant to the inlet of the condensing turbine. Depending on the operating temperature, the remaining thermal energy in stream 2 from desalination plant will be used to generate some electricity rather than totally rejecting to the environment. This integration will increase the power output of the overall system and thus increase the overall exergy efficiency. The third potential example marked by 3 in Fig. 2 is to transfer heat from the heat rejection stages of the desalination plant to heat up the pressurized water in solar thermal power and hydrogen coproduction process. The integration marked by 4 is to transfer heat from solar coproduction process to heat the pressurized brine inlet to the desalination plant. As shown in Fig. 2, depending on operating conditions of thermal desalination plant and solar thermal hydrogen/power production process (Gençer and Agrawal, 2017a; Gençer et al.,2015), there are a number of integration opportunities. Determining the optimum integration is quite challenging. Using the SEWFAC methodology and the modeling approach (Gençer and Agrawal, 2017a), we have systematically synthesized optimal synergistically integrated processes. Furthermore, in conjunction with hydrogen storage and power production around the clock, this integration will provide an opportunity for seawater desalination even when solar energy is not directly available.

3.1. Proposed solar desalination integration approach

There are mainly two large-scale thermal desalination technologies: multi stage flash (MSF) shown in Fig. 3 and multi effect distillation (MED) (Palenzuela et al., 2015; Wu et al., 2013; Shakouri et al., 2010, 2012; Junjie et al., 2007). Both of these systems are operated at low pressures and very close to their saturation temperatures. The first issue regarding the modeling of these systems is the significant discrepancy in reported modeling and simulation results from various studies (Shakouri et al., 2010; Hamed and Aly, 1991; El-Dessouky et al., 1998). To address this issue, detailed process simulation of MSF processes are performed using Aspen Plus and results validated by comparing them with publicly available performance data from the current operating desalination plants such as the Jebel Ali desalination plant in Dubai. We have then examined these process options for improvement opportunities using the SEWFAC process synthesis methodology.

4. Methods

4.1. Process modeling

The detailed simulation of multi stage flash (MSF) thermal desalination process shown in Fig. 3 is performed using Aspen Plus (Tech and Technology, 2006). The electrolyte NRTL (available as ELECNRTL in Aspen Plus), which is a special option for aqueous systems is selected as the base property method to accurately capture dissolution reactions. NBS/NRC steam tables (available as STEAMNBS in Aspen Plus) are used as the free-water method to reflect the water and steam properties in the simulations. The salinity of the feed water is taken to be

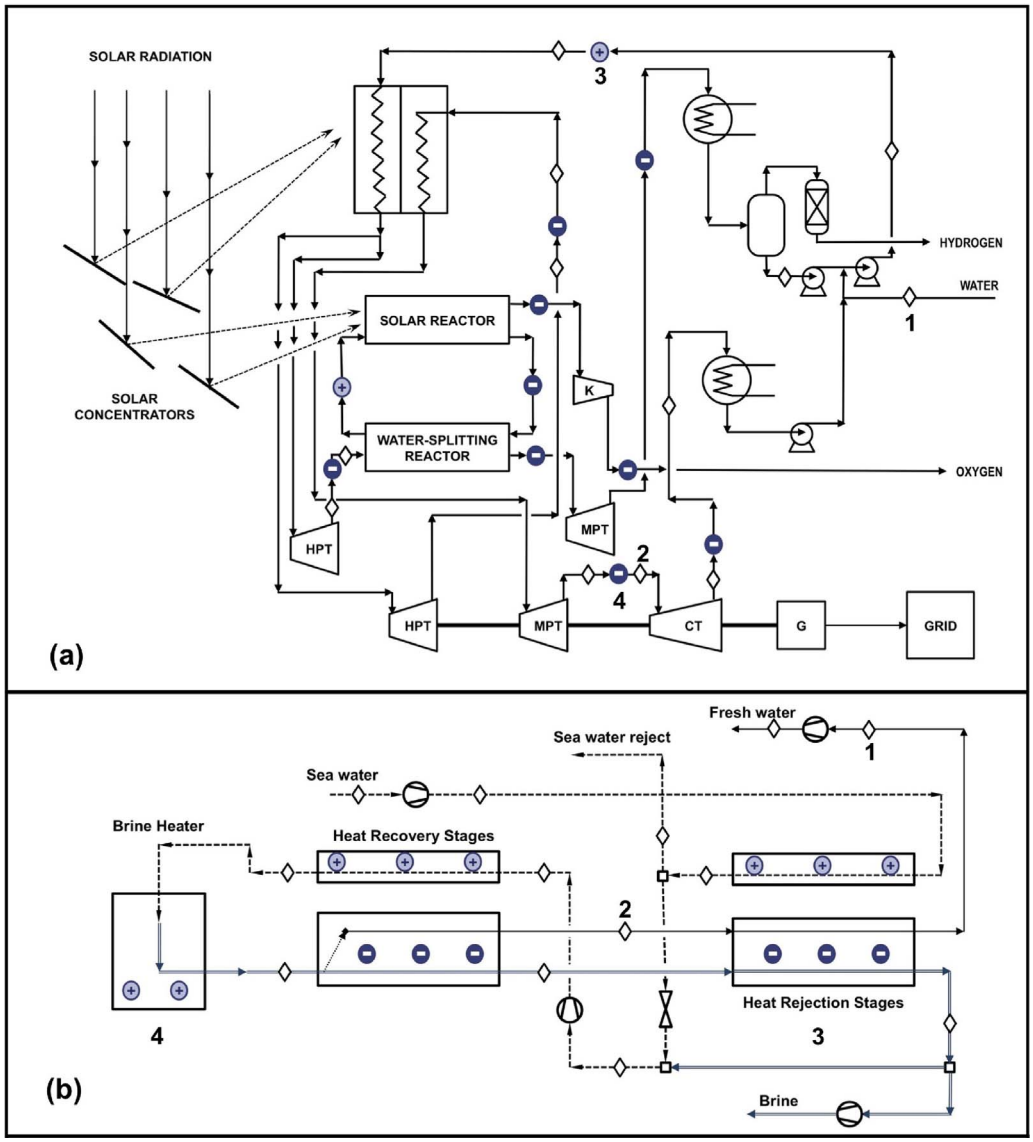

Fig. 2. Potential heat and mass integration points in both processes are marked by minus signed, plus signed circles and diamonds, respectively. (a) Solar thermal hydrogen and electricity production process design. (b) Multi stage flash thermal desalination process flow sheet.

0.040 kg NaCl/kg water (or 40 g NaCl/kg water). Ambient conditions of 35 °C and 1 atm (1.013 bar) are used. Elec Wizard in Aspen Plus is run to accurately predict association and dissociation of Na^+ and Cl^- ions in water solution. A representative MSF desalination process consisting of 16 heat recovery stages and 3 heat rejection stages is considered for this study. Each heat recovery stage contains a heat exchanger and a condensate collector at different pressure corresponding to the boiling point of water at the stage temperature. Heat rejection stages contain heat exchangers to equate the feed and recycled seawater temperature.

As shown in Fig. 3, the saline water is first pumped to 3 bar and fed to the heat rejection section. A portion of the outlet saline water at 2.1 bar and 44 °C is rejected, the remaining portion is depressurized to mix with the recycle brine. The mixed stream reaching salinity of 0.061 kg/kg water is pumped to 7.12 bar, to the inlet condition of the heat recovery stages. The pressurized brine and heated brine are fed counter current to the heat recovery stages. The discharge conditions of pressurized brine stream are 1.36 bar and 98.3 °C. The discharged brine stream is heated to 105 °C at 1.16 bar in the brine heater against steam at 121 °C and 2.1 bar. Fresh water is produced at each stage of the heat recovery section according to the equilibrium vapor fraction of stage's condition. The discharge brine reaches a salinity of 0.069 kg/kg water at 0.118 bar and 49.8 °C. Following the heat rejection stages, a portion of the brine is rejected at 2.4 bar and 42.3 °C and the remaining portion is recycled and mixed with incoming brine at 0.08 bar and 42.3 °C. For 1000 kg/h of saline water feed 134.6 kg/h of fresh water is produced consuming 10.0 kWh thermal energy and 0.41 kWh electricity. Thus, to produce 1 m^3 (or 264.2 gal) of fresh water, the simulated MSF process requires 74.5 kWh thermal energy and 4.1 kWh electricity.

4.2. Integrated process design

All the integrated process designs that are discussed in detail in Section 6 have been modeled and optimized using an integrated Aspen Plus and MATLAB modeling framework. The overall integration steps are shown in Fig. 4. Heat integrations are performed using the Pinch function module developed in MATLAB as part of the modeling framework. We have optimized the process designs based on two objective functions: (i) maximization of heat-to-electricity efficiency while keeping the water to electricity ratio constant, and (ii) maximization of water-to-electricity ratio. In all cases the size of the desalination plant is kept constant. In addition to split fractions of key process streams, the flow rates of electricity and hydrogen production units, and overall heat exchange network are used as decision variables. Operating conditions of process units have not been modified and kept as constraints. The optimization is performed using MATLAB's genetic algorithm, details of the modeling and optimization approach can be found in Gençer and

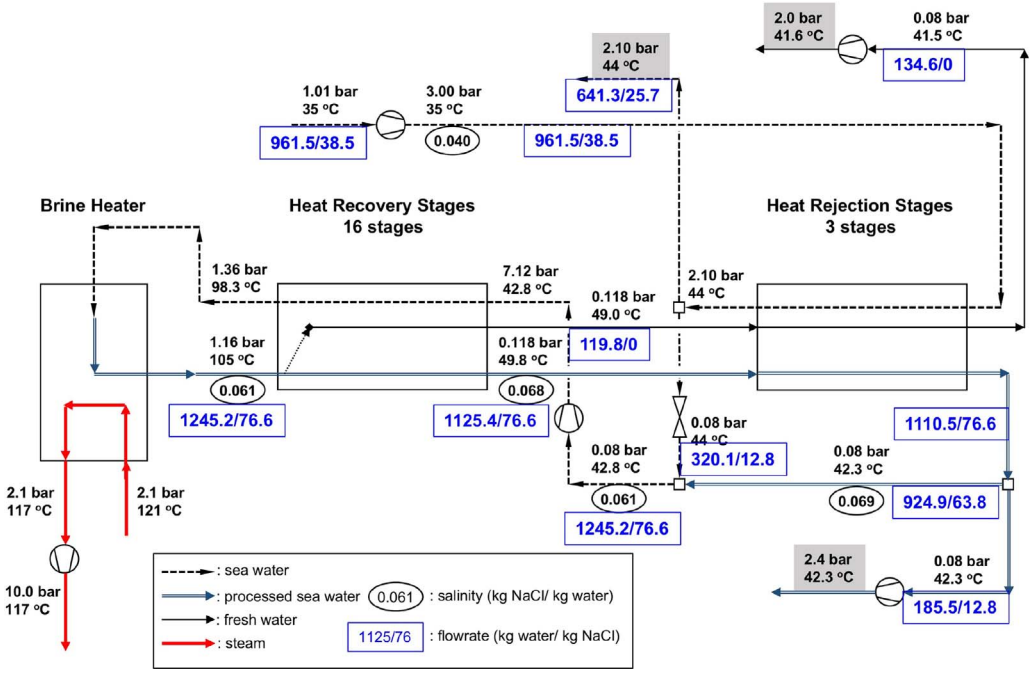

Fig. 3. Standalone multi stage flash (MSF) desalination process flowsheet. The number in elliptical circle is salinity level in kg NaCl/kg water.

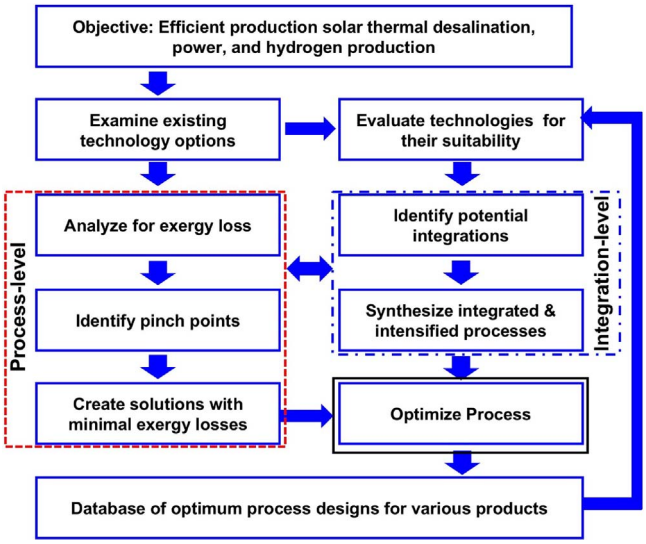

Fig. 4. Methodological steps to perform the proposed integrations.

Agrawal (2017a).

4.3. Metrics

The integrated process designs can be evaluated based on three metrics of interest. water-to-electricity (W/E) ratio (Eq. (1)) demonstrates the relative ratio of fresh water produced from the integrated process.

$$\frac{W}{E} = \frac{V_{\text{fresh water}}\,[\text{m}^3\,\text{h}^{-1}]}{W_{\text{net}}\,[\text{MW}]} \tag{1}$$

Heat-to-electricity (QTE) efficiency (Eq. (2)) shows the conversion of total heat input ($Q_{total,in}$) to the process into electricity (W_{net}), note that it only measures the electricity production of the overall process. This metric is used to understand the effect of fresh water production in reducing the electricity output. A totally synergistic process where only the heat rejected to the environment is used to desalination, QTE efficiency should be equal to the QTE efficiency of the standalone power cycle using the same configuration and operating conditions.

$$\text{QTE} = \frac{W_{\text{net}}}{Q_{\text{total, in}}} \times 100 \tag{2}$$

The Electricity Equivalent Water (EEW, Eq. (3)) is defined as the potential to generate electricity from the thermal energy used for desalination. EEW demonstrates the trade-off value of using thermal energy for fresh water production over power generation. For example, if no thermal MSF was used and only electricity produced from a plant is used for desalination such as RO then this metric provides equivalent electric energy used for desalination. Thus, EEW value provides a direct comparison of any desalination plant such as MSF with an all electric plant such as RO. In Eq. (3), $W_{\text{pot,from }Q}$ is the maximum power that can be generated from given amount of Q using the base power plant model, $V_{\text{fresh water from }Q}$ is the volume of the fresh water produced, $Q_{\text{SWP}-1@\text{T}}$ is the heat requirement of SWP-1 cycle at temperature T, and $\eta_{\text{SWP}-1@\text{T}}$ is the QTE efficiency of SWP-1 cycle at temperature T.

$$\text{EEW} = \frac{W_{\text{pot, from }Q}\,[\text{kWh}]}{V_{\text{fresh water from }Q}\,[\text{m}^3]}, \text{ where}$$
$$W_{\text{pot, from }Q} = (Q_{\text{total, in}} - Q_{\text{SWP}-1@\text{T}}) \times \eta_{\text{SWP}-1@\text{T}}$$
$$\text{and } Q_{\text{SWP}-1@\text{T}} = \frac{W_{\text{net}}}{\eta_{\text{SWP}-1@\text{T}}} \tag{3}$$

5. Integrated desalination process synthesis

In this section, we present various integrated process designs for coproduction of (i) fresh water and electricity, and (ii) fresh water, electricity and hydrogen. First, process steps of current MSF desalination process are unbundled. Second, desalination process is systematically integrated with power and hydrogen production processes. We have also designed and simulated high pressure desalination process designs for electricity coproduction.

5.1. Zones of MSF desalination process

MSF desalination process (MSFDP) is divided into five zones to perform heat and mass integration of the MSF desalination process with solar thermal power generation and hydrogen production processes. Zones Z1–Z3 shown in blue in Fig. 5 are the process units that requires

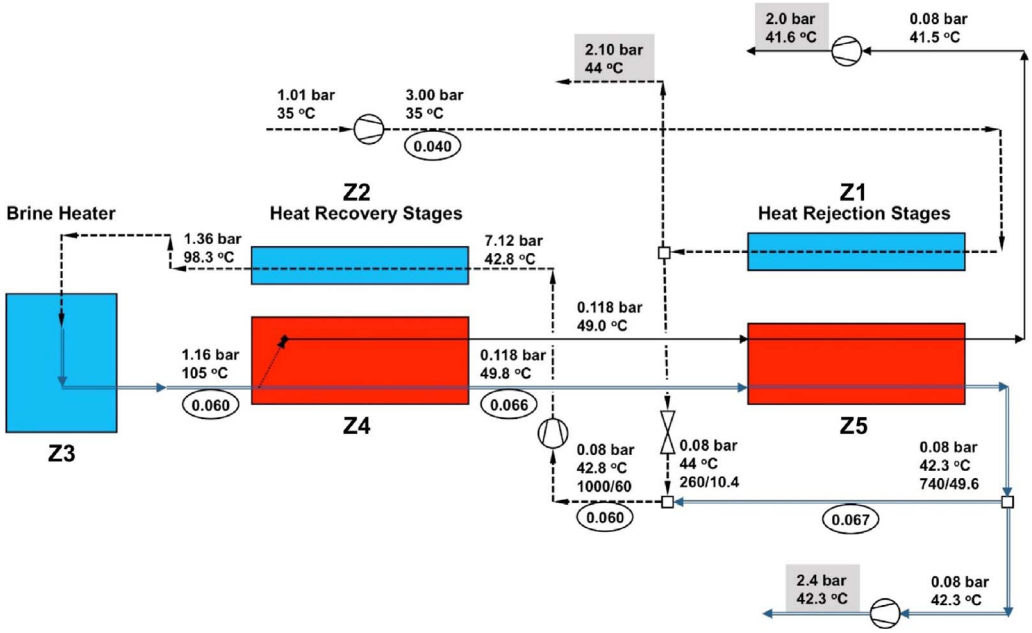

Fig. 5. MSF desalination process split into different zones for heat integration. (For interpretation of the references to color in the text, the reader is referred to the web version of the article.)

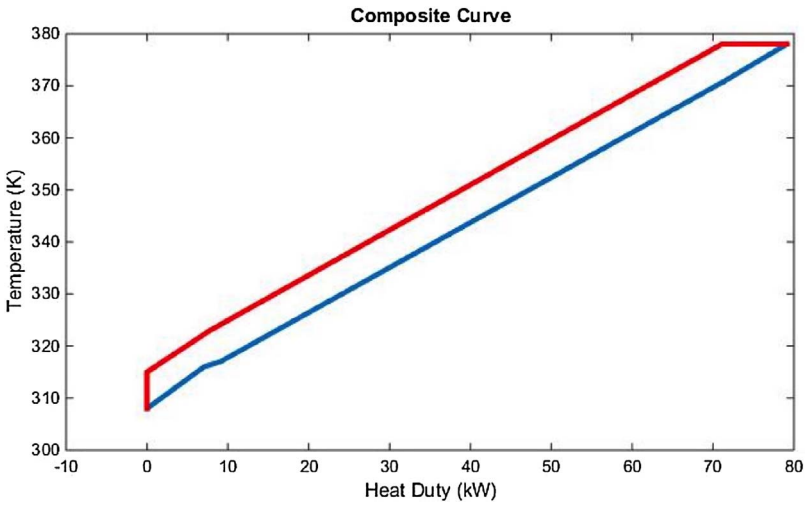

Fig. 6. Composite curve of MSF desalination process shown in Fig. 5.

heat input. Zones Z4 and Z5 shown in red in Fig. 5 are the process units that requires cooling. The heat source of Z3 should be greater than or equal to 121 °C. The temperature levels of other zones are specified in Fig. 5. The standalone MSF desalination process requires 74.5 kWh of thermal energy and 4.1 kWh of electricity per m^3 fresh water produced in standalone operation. The composite curve of the process is shown in Fig. 6. The heat exchange between hot and cold streams are very efficient keeping the temperature difference almost constant throughout the process.

5.2. Solar water power with reheat (SWP-1) cycle integrated with MSF desalination

SWP-1 cycle presented in detail in Gençer and Agrawal (2017b) can be integrated with MSFDP of Fig. 5. The heat exchange units of SWP-1 cycle are shown with blue for heaters and red for coolers in Fig. 7. Two solar heat collection temperatures of 900 K and 1200 K are considered for the integration. 900 K reflects the temperature of the current operational solar thermal power plant while 1200 K is slightly higher, it shows the potential impact of increasing the temperature of operation.

5.3. Modified SWP-1 cycle for improved integration with MSF desalination

The SWP-1 cycle is modified to increase the heat conversion efficiency of the overall process. The modified cycle is designed based on SEWFAC methodology to improve the exergy efficiency of the overall process. The rule applied here is to generate electricity from the highest available temperature in the system before using for other applications. In this case, to improve heat integration the available heat needs to be at different conditions than the ones available in the SWP-1 cycle, hence, to generate those streams, we first start at the highest available temperature and cascade the heat by first generating power. Similar approach is taken in the development of high pressure integrated desalination processes presented in the next sections. The power cycle portion of the integrated process is shown in Fig. 8. The main modification of the power cycle compared to the SWP-1 cycle is the addition of a splitter after the solar heating step. The pressurized superheated steam is split with split fractions of λ_1 and λ_2 ($\lambda_1 + \lambda_2 = 1$). A fraction ($\lambda_1$ for the presented case) is sent through the process units of standard SWP-1 cycle while the remaining fraction is first expanded to a pressure P_4. The expanded stream still has high thermal energy content that is used to supply heating needs of other streams. A pressure adjustment step can be added to lower the pressure to P_5 of the stream after heat

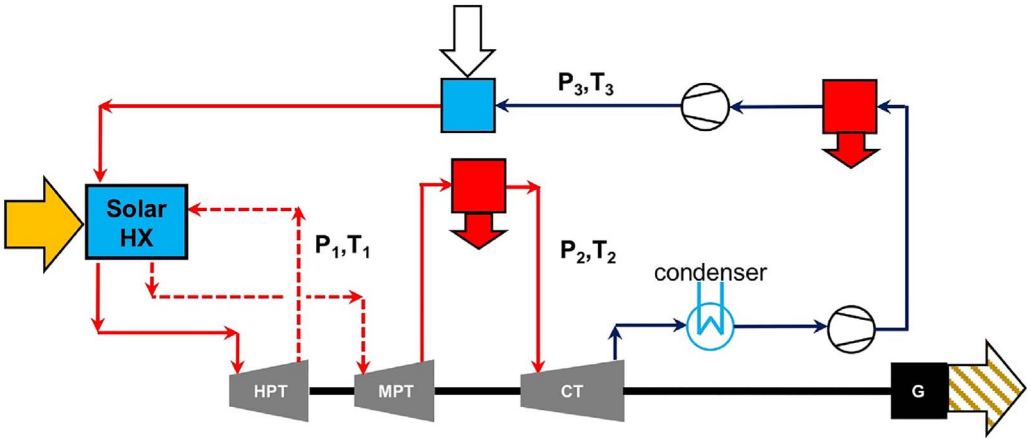

Fig. 7. SWP-1 cycle heat integration zones for integration with MSF desalination process of Fig. 5. Red lines are the water vapor streams, navy blue lines are partially or fully condensed water streams, the operating condition of dashed lines can be optimized, blue rectangles require heat input, and red rectangles are the heat rejecting units. (For interpretation of the references to color in this figure legend, the reader is referred to the web version of the article.)

exchange and it can be further used to heat up process streams. The high pressure high temperature stream used for heating mainly supplies the heat requirement of the intermediate heat exchange step of SWP cycle where pumped water is partially or fully vaporized.

5.4. Continuous solar integrated desalination process

To continuously produce fresh water and electricity, we have integrated MSF desalination process with solar thermal hydrogen and electricity coproduction process or SWH_2P cycle presented in Gençer and Agrawal (2017a) and Gençer et al. (2015a), Gençer et al. (2015b) using the strategy depicted in Fig. 2. Heat exchangers from all three processes are allowed to heat exchange to determine the best integration. Furthermore, the pressurized fresh water will be heated to the highest possible temperature in the system to first generate the maximum electricity from it. Only two-step water splitting with FeO cycle operated at 1600 K reduction temperature and 1000 K oxidation temperature, is considered for the integration (Mallapragada and Agrawal, 2014). These are the optimum operating conditions within the current solar thermal applications as demonstrated in detail in Mallapragada and Agrawal (2014). The produced hydrogen and oxygen will be stored at the same conditions as the hydrogen and oxygen storage of continuous power supply solution presented in Gençer et al. (2015b) and Gençer and Agrawal (2017a). The important part to ensure continuous operation is to convert hydrogen to electricity when solar energy is not available while continuing to produce fresh water. We have used a Hydrogen Water Power (H_2WP) cycle (Gençer and Agrawal, 2017b) integrated with MSF process units.

5.4.1. Hydrogen water power cycle integrated with MSF desalination process

The efficient conversion of hydrogen into electricity while producing desired amount of fresh water is very important. Hence, we have designed a modified H_2WP cycle shown in Fig. 9. The main difference of this cycle is the addition of a heat exchanger after the high pressure turbine. Additionally, we have also allowed heat exchange with medium pressure turbine outlet and condensing turbine outlet. Depending on the optimum process design the discharge stream of the medium pressure turbine can be split and while a portion is directed to condensing turbine, the remaining portion can be used for heat exchange only. The fraction (λ_1 and $\lambda_2 = 1 - \lambda_1$) for either path varies between 0 and 1.

5.5. High pressure integrated desalination process

Current thermal desalination processes are designed and operated at very low pressures. This is mainly due to minimize the increased corrosive effect of seawater at high pressures. To investigate the potential of high pressure operation, we have studied several process designs for coproduction of electricity and fresh water. Integrated desalination process design presented in Fig. 10 is a high pressure fresh water and power production process. The details of the process for operating pressure of 200 bar and solar heat collection temperature of 1600K (or 1327 °C) is given in Table 1.

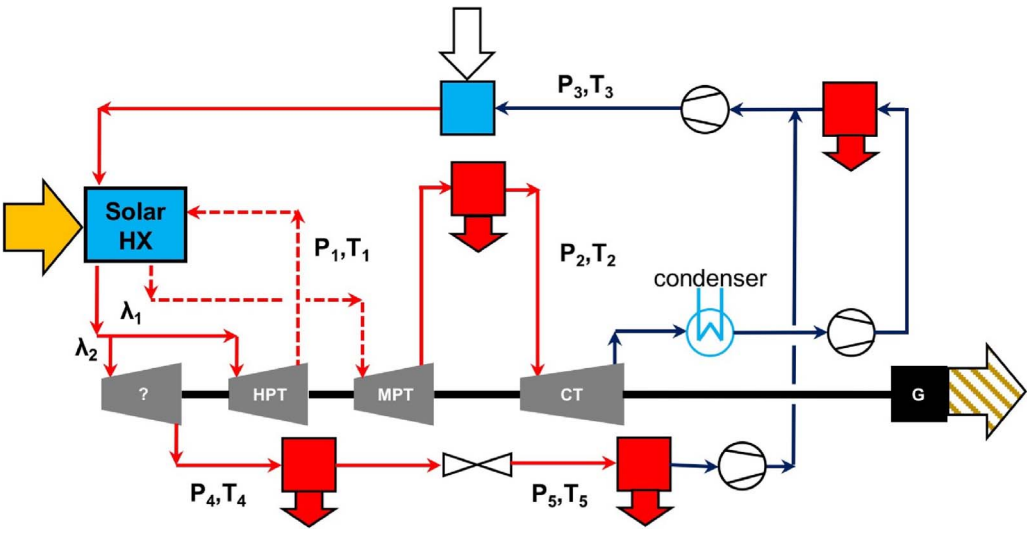

Fig. 8. Modified SWP-1 cycle heat integration zones for integration with MSF desalination process of Fig. 5.

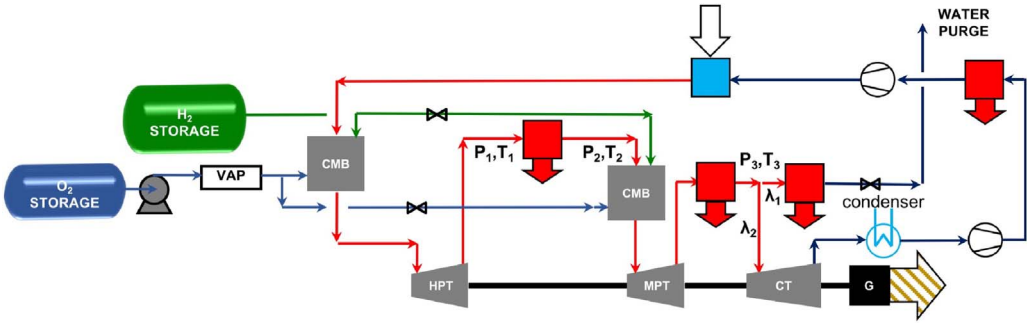

Fig. 9. Modified Hydrogen Water Power cycle heat integration zones for integration with MSF desalination process of Fig. 5. VAP: O_2 vaporization, CMB: combustion chamber, HPT: high pressure turbine, MPT: medium pressure turbine, CT: condensing turbine, G: generator. Red lines: steam streams, navy blue lines: partially or fully condensed water streams, green lines: hydrogen streams, blue lines: oxygen streams. (For interpretation of the references to color in this figure legend, the reader is referred to the web version of the article.)

5.6. Hybrid high pressure–low pressure integrated desalination process

In another novel configuration shown in Fig. 11, we have integrated high pressure desalination process proposed in the previous section with a regular low pressure MSF desalination process. The integration is performed by using the exhaust (stream S_6 in Fig. 11) of the dense fluid expander as the vaporized brine input to the regular MSF desalination process. With this integration, fresh water production at high pressure and high temperature is completed by low pressure and low temperature operation while the fresh water produced at high temperature as steam is used to generate power. This hybrid process design aims to increase the fresh water production from a given amount of solar heat. The integration is performed by adjusting the pressure of the brine leaving the high pressure desalination part of the process and reducing its pressure through a dense fluid expander. The stream is then fed to MSF desalination process units to further produce fresh water. The details of the process for operating pressure of 200 bar and solar heat collection temperature of 1600 K (or 1327 °C) is given in Tables 2 and 3.

Table 1
Details of high pressure integrated desalination process of Fig. 10.

Stream	Temperature [°C]	Pressure [bar]	Salinity [kg/kg water]
S1	35	1.01	0.040
S2	35	200	0.040
S3	368	200	0.052
S4	361	180	0.076
S5	200	180	0.076
S6	135	3	0.076
S7	135	3	0.086
S8	40	3	0.086
S9	135	3	0.000
S10	40	3	0.000
S11	368	200	0.076
S12	361	180	0.000
S13	1327	180	0.000
S14	855	15.5	0.000
S15	848	1.2	0.000
S16	110	1.2	0.000
S17	41	0.08	0.000
S18	40	2	0.000

6. Results and discussion

W/E ratio is an important characteristic of the process since generally, water need is much higher than the electricity need of a region. In designing an integrated desalination plant, the most convenient scheme is to use waste heat from a process such as power plant. However, due to enormous water demand, using waste heat alone is often times unable to meet the heat requirement to produce the desired amount of fresh water. The capacity of Jebel Ali M-Station is used as basis for the evaluation of integrated solar desalination process designs. Jebel Ali M-Station, UAE's biggest power production and desalination plant, has an installed electricity generation capacity of ~2060 MW and fresh water production capacity of 140 million gallons of water per day (529,957.6 m^3/day). For all calculations, the power supply of 2060 MW is assumed and the relative fresh water production is calculated accordingly. W/E ratio of Jebel Ali plant is 10.7 m^3/h/MW.

For the SWP-1 integration (Fig. 7), if the main focus of plant is to produce power, the rejected heat is unable to meet the water production ratio expected from a combined plant as summarized in Table 4. The electricity generation capacity from the thermal energy used for desalination is pretty low since the fresh water production is very low, about 2% of our base case. The composite curve for the SWP-1 cycle integration operated at 1200 K, shown in Fig. 12, demonstrates that the heat requirement of the desalination is met by the intermediate heat exchange step, which increased the overall solar energy input. Additional solar energy input is to make up for the reduced intermediate heat exchange that preheats the pumped water prior to solar heat

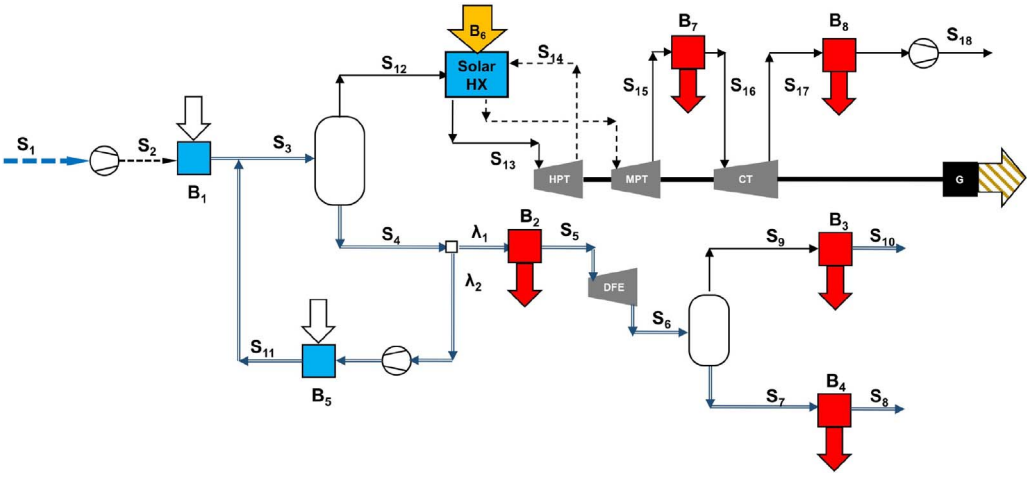

Fig. 10. High pressure desalination and electricity coproduction process design. Blocks B_1, B_2, etc. represent various heat exchangers/collectors. Streams S_{10} and S_{18} represent desalinated water and S_8 salt rejection stream. G is electricity generated. DEE is dense fluid expander.

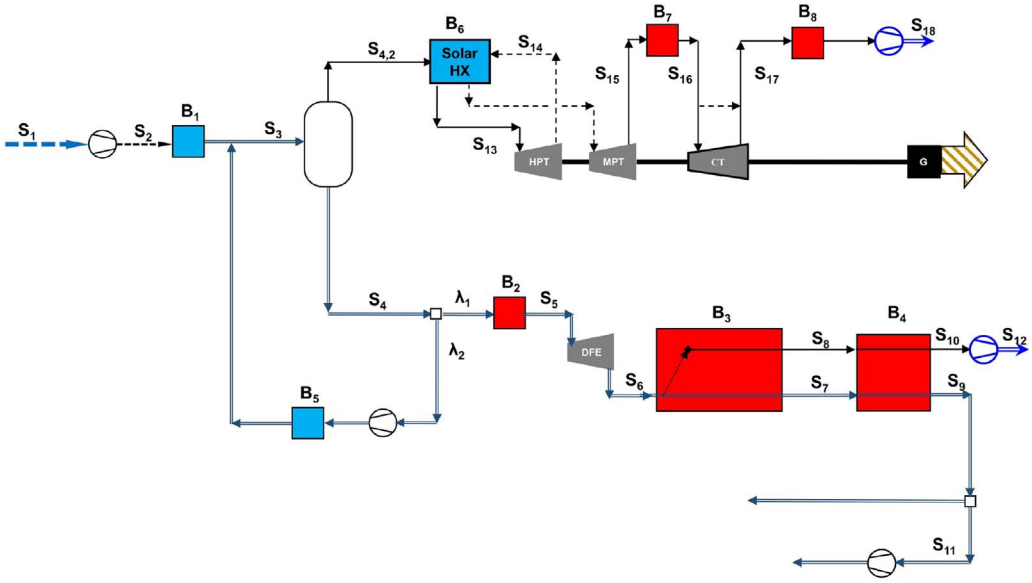

Fig. 11. Hybrid high pressure–low pressure desalination and electricity coproduction process design.

Table 2
Stream details of hydrid high pressure–low pressure integrated desalination process of Fig. 11.

Stream	Temperature [°C]	Pressure [bar]	Salinity [kg/kg water]
S1	35	1.01	0.040
S2	35	200	0.040
S3	368	200	0.042
S4	366	195	0.042
S5	105	195	0.042
S6	105	1.16	0.042
S7	49.6	0.118	0.049
S8	49.03	0.118	0.000
S9	42.0	0.08	0.050
S10	41.44	0.08	0.000
S11	42.0	0.08	0.050
S12	42.0	2.1	0.000
S13	1327	195	0.000
S14	842	15.5	0.000
S15	848	1.2	0.000
S16	110	1.2	0.000
S17	41	0.08	0.000
S18	40	2	0.000

Table 3
Block details of hybrid high pressure–low pressure integrated desalination process of Fig. 11 for production of 90 kW of electricity and 0.247 m^3/h of fresh water. Negative and positive numbers refer to heat added or removed, respectively.

Block	Heat duty [kW]
B1	−418
B2	+314
B3	+44.4
B4	+5.0
B5	−2.29
B6	−56.98
B6r	−26.22
B7	+33.46
B8	+47.12

exchanger. We observe this shift in utilization of heat in the reduced heat-to-electricity efficiency of the cycle 47.8% relative to 49.9% for standalone SWP-1 cycle. EEW value for these integration are quite high 153.1 kWh/m^3 relative to 4–10 kWh/m^3 of RO desalination as the fresh water production is extremely low.

Table 4
SWP-1 cycle integration with power generation focus.

T [K]	W/E ratio [m^3/h/MW]	Heat-to-electricity efficiency [%]	EEW [kWh/m^3]
900	0.25	40.8	158.8
1200	0.19	47.8	153.1

When the objective of the integration is to keep the W/E ratio, additional heat is required not only to make-up for the reduced intermediate heat exchange but also to operate the desalination process, see Fig. 13 and Table 5. The heat-to-electricity efficiency of the integrated system is 40.1% and 44.9% for operation at 1200 K and 1600 K, respectively. The EEW values are also higher compared to the previous case with 22.2 kWh/m^3 and 23.8 kWh/m^3 for 1200 K and 1600 K cases, respectively. This outcome is a result of supplying additional heat requirement at the solar heat collection temperatures of 1200 K and 1600 K where as the temperature level required to run the desalination plant is close to 400 K.

The modified SWP-1 cycle (Fig. 8) achieves higher heat-to-electricity of 51.1% for W/E ratio of 10.2 m^3/h/MW with EEW value of 9.2 kWh/m^3 at 1600 K (Table 5). At 1200 K although the heat-to-electricity efficiency drops to 45.6%, EEW value also reduces to 7.7 kWh/m^3. The higher performance is due to the better heat integration of the process as shown in the composite curve of Fig. 14. With the modified configuration, the thermal energy at solar heat collection temperature is first used to generate power and then as a heat source to run the desalination process units. The MSF desalination process heat requirement is met by the condensation of the steam at intermediate pressure level as can be observed from Fig. 14.

Although high pressure integrated desalination process (Fig. 10) can yield heat-to-electricity efficiency of 53.3% and 52.3% if the dense fluid expander (DEE in Fig. 10) is not used, the maximum achievable W/E ratio is low. The W/E ratio varies from 1.41 m^3/h/MW to 1.81 m^3/h/MW. This translates into meeting up to 16.4% of the fresh water production capacity expected from a large scale facility. However, this process can be further heat integrated with the MSF desalination process (Fig. 11). Such an integration further benefits from low temperature and low pressure vaporized brine to run a MSF desalination process and can reach W/E ratio of 10.1 m^3/h/MW with a heat-to-electricity efficiency of 47.7% and EEW value of 17 kWh/m^3.

The power and fresh water coproduction process alternatives provide efficient solution for solar energy utilization. However, continuous

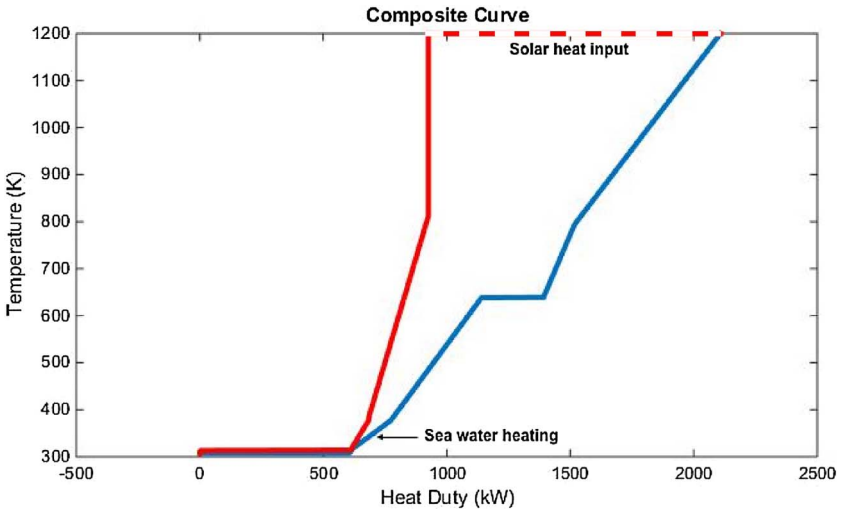

Fig. 12. Composite curve for SWP-1 cycle integrated with MSF desalination process operated at 1200 K solar heat collection temperature.

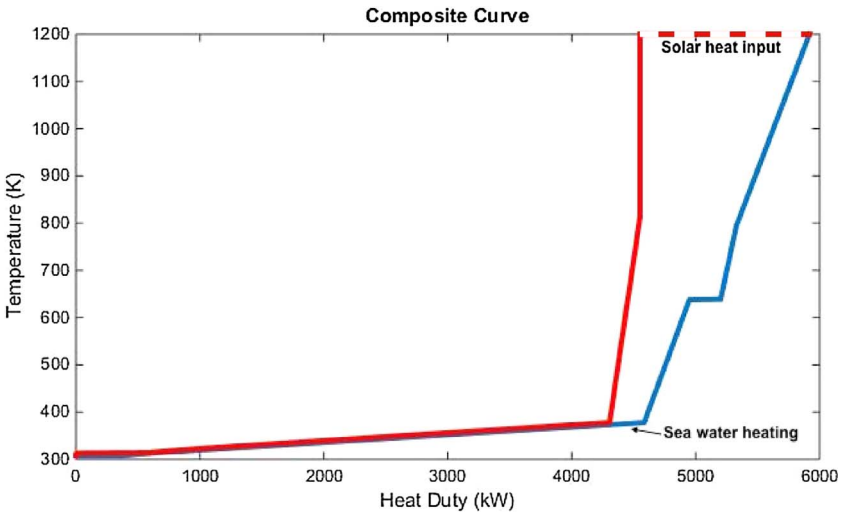

Fig. 13. Composite curve for SWP-1 cycle integrated with MSF desalination process to meet the desired W/E ratio operated at 1200 K solar heat collection temperature.

Table 5
SWP-1 and modified SWP-1 cycle integration for a W/E ratio of 10.2 m^3/h/MW.

	T [K]	Heat-to-electricity efficiency [%]	EEW [kWh/m^3]
SWP-1	1200	40.1	22.2
SWP-1	1600	44.9	23.8
Modified SWP-1	1200	45.6	7.7
Modified SWP-1	1600	51.1	9.2

operation of the plant is critical to keep the performance of the process at its optimum value and maximize the utilization of equipment. Continuous solar integrated desalination process coproduces hydrogen, electricity and fresh water during daytime. Produced hydrogen and oxygen are stored and utilized to run the modified hydrogen power cycle to continue producing electricity and fresh water during night time. For a W/E ratio of 11 m^3/h/MW, the overall heat-to-electricity efficiency is 36.5%. The optimum process design for coproduction of hydrogen and electricity (without fresh water production) achieved heat-to-electricity efficiency of 44.0% for the same operating conditions (Gençer et al., 2015b). The composite curve of the overall daytime cycle is shown in Fig. 15. EEW for the cycle at W/E of 11 m^3/h/MW is calculated to be 18.7 kWh/m^3. The coproduction strategy reduces the total heat input by 11.7% compared to the sum of standalone processes that produce the same outputs. Hence, overall integration of thermal desalination processes with hydrogen and electricity production is a synergistic alliance.

7. Conclusion

In this study, using SEWFAC process synthesis concept, we have identified synergistic integrations between solar thermal power and hydrogen production processes and MSF desalination process. These process designs can meet the water demand with rather high conversion efficiencies. There are a vast number of opportunities in desalination field to apply SEWFAC approach for example integration with other desalination processes such as electricity-driven alternatives. Moreover, a new metric, Electricity Equivalent Water (EEW), is proposed to evaluate the performance of the desalination process from power point of view. The usually very high thermal energy consumption values can be misleading without considering the temperature level of the heat used to run the process. EEW accounts for the temperature level by calculating the maximum achievable electricity generation from the thermal energy dedicated to desalination process. EEW value is in the vicinity of ~22 kWh/m^3 for direct integration of MSF desalination with SWP-1. However, the performance can be highly improved for integration with modified SWP-1 cycle that has a EEW value in the range of 7.7 and 9.2 kWh/m^3, which is close to the RO electricity requirement of 4–10 kWh/m^3. Furthermore, the triproduction process can be further integrated with a hydrogen power cycle, to continue the electricity and fresh water production continuously. The round-the-clock operation yields 36.5% heat-to-electricity efficiency and provides more than 11%

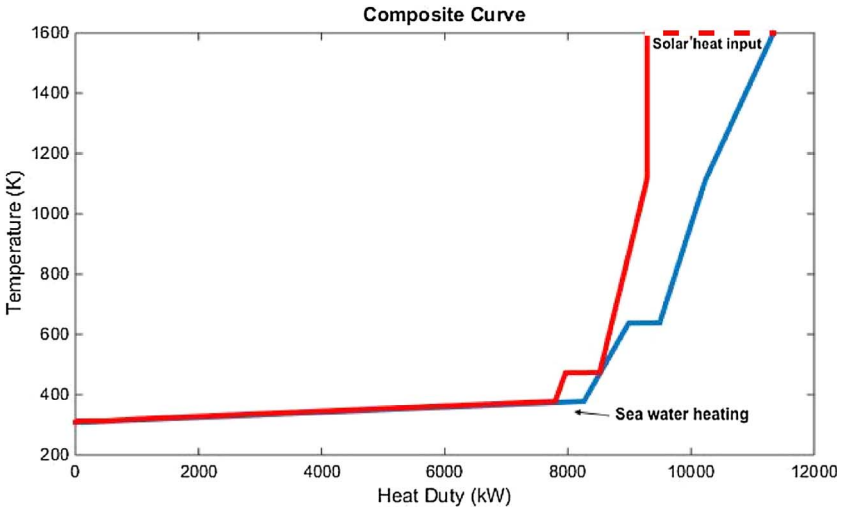

Fig. 14. Composite curve for modified SWP cycle integrated with MSF desalination process to meet the desired W/E ratio operated at 1600 K solar heat collection temperature.

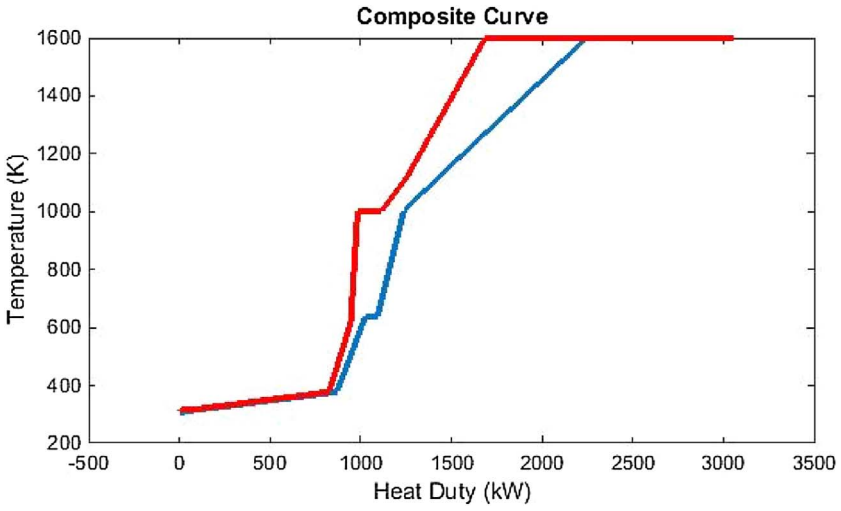

Fig. 15. Day-time composite curve for SWH_2P cycle integrated with MSF desalination process to meet the desired W/E ratio operated at 1600 K solar heat collection temperature.

thermal energy savings compared to the sum of standalone processes. The presented process designs with desired W/E ratio and high conversion efficiencies are promising solutions for sustainable fresh water supply.

Acknowledgments

Research supported as part of the Center for Direct Catalytic Conversion of Biomass to Biofuels, an Energy Frontier Research Center funded by U.S. Department of Energy, Office of Science, Basic Energy Sciences (BES), under Award DE-SC SC0000997; by the National Science Foundation Solar Economy IGERT (0903670-DGE).

References

Agrawal, R., Mallapragada, D.S., 2010. Chemical engineering in a solar energy-driven sustainable future. AIChE J. 56 (11), 2762–2768. http://dx.doi.org/10.1002/aic.12435.

Agrawal, R., Singh, N.R., 2010. Solar energy to biofuels. Annu. Rev. Chem. Biomol. Eng. 1 (1), 343–364. http://dx.doi.org/10.1146/annurev-chembioeng-073009-100955.

Alexandratos, N., Bruinsma, J., 2012. World agriculture towards 2030/2050. Tech. Rep. 4. Agricultural Development Economincs Division Food and Agriculture Organization of the United Nationshttp://dx.doi.org/10.1016/S0264-8377(03)00047-4.

Al-musleh, E.I., Mallapragada, D.S., Agrawal, R., 2014. Continuous power supply from a baseload renewable power plant. Appl. Energy 122, 83–93.

Ben Bacha, H., Dammak, T., Ben Abdalah, A.A., Maalej, A.Y., Ben Dhia, H., 2007. Desalination unit coupled with solar collectors and a storage tank: modelling and simulation. Desalination 206 (1–3), 341–352. http://dx.doi.org/10.1016/j.desal.2006.05.018.

BP statistical review of world energy. Tech. Rep. BP.

Carlton, J.S., Mase, A.S., Knutson, C.L., Lemos, M.C., Haigh, T., Todey, D.P., Prokopy, L.S., 2016. The effects of extreme drought on climate change beliefs, risk perceptions, and adaptation attitudes. Clim. Change 135 (2), 211–226. http://dx.doi.org/10.1007/s10584-015-1561-5.

Chang, H., Lyu, S.-G., Tsai, C.-M., Chen, Y.-H., Cheng, T.-W., Chou, Y.-H., 2012. Experimental and simulation study of a solar thermal driven membrane distillation desalination process. Desalination 286, 400–411. http://dx.doi.org/10.1016/j.desal.2011.11.057.

Duran, M.A., Grossmann, I.E., 1986. Simultaneous optimization and heat integration of chemical processes. AIChE J. 32 (1), 123–138. http://dx.doi.org/10.1002/aic.690320114.

EIA, 2015. Annual energy outlook 2015 with projections to 2040, Report DOE/EIA-0383(2015) %!. U.S. Energy Information Administration.

El-Dessouky, H., Alatiqi, I., Ettouney, H., 1998. Process synthesis: the multi-stage flash desalination system. Desalination 115 (2), 155–179. http://dx.doi.org/10.1016/S0011-9164(98)00035-6.

El-Halwagi, M.M., 2006. Process Integration, vol. 7 Academic Press.

El-Halwagi, M.M., Manousiouthakis, V., 1989. Synthesis of mass exchange networks. AIChE J. 35 (8), 1233–1244. http://dx.doi.org/10.1002/aic.690350802.

FAO, 2015. World Fertilizer Trends and Outlook to 2018.

Favrat, D., Marechal, F., 2015. Exergy representations in thermodynamics. HEFAT 2015.

Field, C.B., Michalak, A.M., 2015. Water, climate, energy, food: inseparable & indispensable. Daedalus 144 (3), 7–17. http://dx.doi.org/10.1162/DAED_a_00337.

Floudas, C.A., Elia, J.A., Baliban, R.C., 2012. Hybrid and Single Feedstock Energy Processes for Liquid Transportation Fuels: A Critical Review. http://dx.doi.org/10.1016/j.compchemeng.2012.02.008.

Garcia, D., You, F., 2017. Systems engineering opportunities for agricultural and organic waste management in the food-water-energy nexus. Curr. Opin. Chem. Eng. 18, 23–31. http://dx.doi.org/10.1016/j.coche.2017.08.004.

Gençer, E., Agrawal, R., 2016. A commentary on the US policies for efficient large scale renewable energy storage systems: focus on carbon storage cycles. Energy Policy 88 (C), 477–484. http://dx.doi.org/10.1016/j.enpol.2015.11.003 0301-4215/.

Gençer, E., Agrawal, R., 2017a. Strategy to synthesize integrated solar energy

coproduction processes with optimal process intensification. Case study: efficient solar thermal hydrogen production. Comput. Chem. Eng. 105, 328–347. http://dx.doi.org/10.1016/j.compchemeng.2017.01.038.
Gençer, E., Agrawal, R., 2017b. Synthesis of efficient solar thermal power cycles for baseload power supply. Energy Convers. Manag. 133, 486–497. http://dx.doi.org/10.1016/j.enconman.2016.10.068.
Gençer, E., Al-musleh, E., Mallapragada, D.S., Agrawal, R., 2014a. Uninterrupted renewable power through chemical storage cycles. Curr. Opin. Chem. Eng. 5, 29–36. http://dx.doi.org/10.1016/j.coche.2014.04.001.
Gençer, E., Mallapragada, T.M., Dharik, S., Agrawal, R., 2014b. Synergistic biomass and natural gas conversion to liquid fuel with reduced CO_2 emissions. Comput. Aided Chem. Eng. 34, 525–530. http://dx.doi.org/10.1016/B978-0-444-63433-7.50072-9.
Gençer, E., Tawarmalani, M., Agrawal, R., 2015a. Integrated solar thermal hydrogen and power coproduction process for continuous power supply and production of chemicals. Comput. Aided Chem. Eng. 37, 2291–2296. http://dx.doi.org/10.1016/B978-0-444-63576-1. 50076-5.
Gençer, E., Mallapragada, D.S., Maréchal, F., Tawarmalani, M., Agrawal, R., François, M., Mohit, T., Rakesh, A., 2015b. Round-the-clock power supply and a sustainable economy via synergistic integration of solar thermal power and hydrogen processes. Proc. Natl. Acad. Sci. U. S. A. 112 (52), 15821–15826. http://dx.doi.org/10.1073/pnas.1513488112.
Gençer, E., Miskin, C., Sun, X., Khan, M.R., Bermel, P., Ashraf Alam, M., Agrawal, R., 2017. Directing solar photons to sustainably meet food, energy, and water needs. Sci. Rep. 7, 3133. http://dx.doi.org/10.1038/s41598-017-03437-x.
Gonzlez-Bravo, R., Npoles-Rivera, F., Ponce-Ortega, J.M., Nyapathi, M., Elsayed, N., El-Halwagi, M.M., 2015. Synthesis of optimal thermal membrane distillation networks. AIChE J. 61 (2), 448–463. http://dx.doi.org/10.1002/aic.14652.
Gonzlez-Bravo, R., Ponce-Ortega, J.M., El-Halwagi, M.M., 2017. Optimal design of water desalination systems involving waste heat recovery. Ind. Eng. Chem. Res. 56 (7), 1834–1847. http://dx.doi.org/10.1021/acs.iecr.6b04725.
Gude, V.G., Nirmalakhandan, N., Deng, S., 2010. Renewable and sustainable approaches for desalination. Renew. Sustain. Energy Rev. 14 (9), 2641–2654. http://dx.doi.org/10.1016/j.rser.2010.06.008.
Guerra, O.J., Caldern, A.J., Papageorgiou, L.G., Siirola, J.J., Reklaitis, G.V., 2016. An optimization framework for the integration of water management and shale gas supply chain design. Comput. Chem. Eng. 92, 230–255. http://dx.doi.org/10.1016/j.compchemeng.2016.03.025. http://www.sciencedirect.com/science/article/pii/S0098135416300874.
Hamed, O.A., 2005. Overview of hybrid desalination systems – current status and future prospects. Desalination 186 (1–3), 207–214. http://dx.doi.org/10.1016/j.desal.2005.03.095.
Hamed, O.A., Aly, S., 1991. Simulation and design of MSF desalination processes. Desalination 80 (1), 1–14. http://dx.doi.org/10.1016/0011-9164(91)80001-C.
Hernández, B., Martín, M., 2017. Optimal integrated plant for production of biodiesel from waste. ACS Sustain. Chem. Eng. 5 (8), 6756–6767. http://dx.doi.org/10.1021/acssuschemeng.7b01007.
Hoekstra, A.Y., Mekonnen, M.M., 2012. The water footprint of humanity. Proc. Natl. Acad. Sci. U. S. A. 109 (9), 3232–3237. http://dx.doi.org/10.1073/pnas.1109936109. arXiv:1408.1149.
IPCC, 2014. Summary for Policymakers. http://dx.doi.org/10.1017/CBO9781107415324. arXiv:1011.1669v3.
Jemmali, H., Sullivan, C.A., 2014. Multidimensional analysis of water poverty in MENA region: an empirical comparison with physical indicators. Soc. Indic. Res. 115 (1), 253–277. http://dx.doi.org/10.1007/s11205-012-0218-2.
Junjie, Y., Shufeng, S., Jinhua, W., Jiping, L., 2007. Improvement of a multi-stage flash seawater desalination system for cogeneration power plants. Desalination 217 (1–3), 191–202. http://dx.doi.org/10.1016/j.desal.2007.02.016.
Kalogirou, S., 1998. Use of parabolic trough solar energy collectors for sea-water desalination. Appl. Energy 60 (2), 65–88. http://dx.doi.org/10.1016/S0306-2619(98)00018-X.
Kucera, J., 2014. Desalination. John Wiley & Sons, Inc., Hoboken, NJ, USA. http://dx.doi.org/10.1002/9781118904855.
Lam, K.L., Lant, P.A., O'Brien, K.R., Kenway, S.J., 2016. Comparison of water-energy trajectories of two major regions experiencing water shortage. J. Environ. Manag. 181, 403–412. http://dx.doi.org/10.1016/j.jenvman.2016.06.068.
Larsen, M.A.D., Drews, M., Gani, R., 2016. Water consumption in the energy sector. Dtu International Energy Report 2016: the energy–water–food nexus – from local to global aspects.
Li, C., Goswami, Y., Stefanakos, E., 2013. Solar assisted sea water desalination: a review. Renew. Sustain. Energy Rev. 19, 136–163. http://dx.doi.org/10.1016/j.rser.2012.04.059. http://www.sciencedirect.com/science/article/pii/S136403211200617X.
Liu, J., Yang, H., Gosling, S.N., Kummu, M., Flörke, M., Hanasaki, N., Wada, Y., Zhang, X., Zheng, C., 2017. Water scarcity assessments in the past, present, and future. Earth's Future 1–15. http://dx.doi.org/10.1002/eft2.200.
Mallapragada, D.S., Agrawal, R., 2014. Limiting and achievable efficiencies for solar thermal hydrogen production. Int. J. Hydrogen Energy 39 (1), 62–75. http://dx.doi.org/10.1016/j.ijhydene.2013.10.075.
Mallapragada, D.S., Tawarmalani, M., Agrawal, R., 2014. Synthesis of augmented biofuel processes using solar energy. AIChE J. 60 (7), 2533–2545. http://dx.doi.org/10.1002/aic.14456.
Mathioulakis, E., Belessiotis, V., Delyannis, E., 2007. Desalination by using alternative energy: review and state-of-the-art. Desalination 203 (1–3), 346–365 doi:10.1016/j.desal.2006.03.531|10.1016/j.desal.2006.06.531.
Maupin, M.A., Kenny, J.F., Hutson, S.S., Lovelace, J.K., Barber, N.L., Linsey, K.S., 2014. Estimated Use of Water in the United States in 2010: U.S. Geological Survey Circular 1405. Tech. Rep. http://dx.doi.org/10.3133/cir1405. Reston, VA.
MENA, 2011. Regional Water Outlook: Part II Desalination Using Renewable Energy. Tech. Rep. March, DLR. doi:6543P07/FICHT-7109954-v2.
Molden, D., 2007. Water for Food, Water for Life: A Comprehensive Assessment of Water Management in Agriculture. Earthscan, London. http://dx.doi.org/10.1007/s10795-008-9044-8.
Moser, M., Trieb, F., Kern, J., 2010. Combined water and electricity production on industrial scale in the MENA countries with concentrating solar power. Desalination 286, 358–371.
Palenzuela, P., Zaragoza, G., Alarcón-Padilla, D.C., Guillén, E., Ibarra, M., Blanco, J., Alarcon-Padilla, D.C., Guillen, E., Ibarra, M., Blanco, J., 2011a. Assessment of different configurations for combined parabolic-trough (PT) solar power and desalination plants in arid regions. Energy 36 (8), 4950–4958. http://dx.doi.org/10.1016/j.energy.2011.05.039.
Palenzuela, P., Zaragoza, G., Alarcon, D., Blanco, J., 2011b. Simulation and evaluation of the coupling of desalination units to parabolic-trough solar power plants in the Mediterranean region. Desalination 281, 379–387. http://dx.doi.org/10.1016/j.desal.2011.08.014.
Palenzuela, P., Alarcon-Padilla, D.C., Zaragoza, G., 2015. Large-scale solar desalination by combination with CSP: techno-economic analysis of different options for the Mediterranean Sea and the Arabian Gulf. Desalination 366, 130–138. http://dx.doi.org/10.1016/j.desal.2014.12.037.
Palmer, M.A., Liu, J., Matthews, J.H., Mumba, M., D'Odorico, P., 2015. Manage water in a green way. Science 349 (6248), 584–585. http://dx.doi.org/10.1126/science.aac7778.
Qiblawey, H.M., Banat, F., 2008. Solar thermal desalination technologies. Desalination 220 (1–3), 633–644. http://dx.doi.org/10.1016/j.desal.2007.01.059.
Ramapriya, G.M., Tawarmalani, M., Agrawal, R., 2014. Modified basic distillation configurations with intermediate sections for energy savings. AIChE J. 60 (3), 1091–1097. http://dx.doi.org/10.1002/aic.14324.
Salcedo, R., Antipova, E., Boer, D., Jiménez, L., Guillén-Gosálbez, G., 2012. Multi-objective optimization of solar Rankine cycles coupled with reverse osmosis desalination considering economic and life cycle environmental concerns. Desalination 286, 358–371. http://dx.doi.org/10.1016/j.desal.2011.11.050.
Shakouri, M., Ghadamian, H., Sheikholeslami, R., 2010. Optimal model for multi effect desalination system integrated with gas turbine. Desalination 260 (1–3), 254–263. http://dx.doi.org/10.1016/j.desal.2010.03.032.
Shakouri, M., Ghadamian, H., Bagheri, F.M., 2012. Feasibility study of integrating multi effect desalination and gas turbine systems for Lavan island oil refinery. Iran. J. Chem. Chem. Eng. – Int. Engl. Ed. 31 (3), 115–124.
Shatat, M., Worall, M., Riffat, S., 2013. Opportunities for solar water desalination worldwide: review. Sustain. Cities Soc. 9, 67–80. http://dx.doi.org/10.1016/j.scs.2013.03.004. https://www.sciencedirect.com/science/article/pii/S2210670713000176.
Shenvi, A.A., Shah, V.H., Agrawal, R., 2013. New multicomponent distillation configurations with simultaneous heat and mass integration. AIChE J. 59 (1), 272–282. http://dx.doi.org/10.1002/aic.13971.
Slocum, A.H., Codd, D.S., Buongiorno, J., Forsberg, C., McKrell, T., Nave, J.-C., Papanicolas, C.N., Ghobeity, A., Noone, C.J., Passerini, S., Rojas, F., Mitsos, A., 2011. Concentrated solar power on demand. Sol. Energy 85 (7), 1519–1529. http://dx.doi.org/10.1016/j.solener.2011.04.010.
Tech, A., Technology, A., 2006. ASPEN Plus users guide. Report. Aspen Technology Inc., Burlington, MA.
The Water Project. https://thewaterproject.org/ (access date: 12.09.17).
Tock, L., Maréchal, F., 2015. Thermo-environomic optimisation strategy for fuel decarbonisation process design and analysis. Comput. Chem. Eng. 83, 110–120. http://dx.doi.org/10.1016/j.compchemeng.2015.04.018.
United Nations Food and Agricultural Organization (FAO), 2011. The State of the World's Land and Water Resources for Food and Agriculture: Managing Systems at Risk. New York.
Vorosmarty, C., Green, P., Salisbury, J., Lammers, R., 2000. Global water resources: vulnerability from climate change and population growth. Science 289 (JULY), 284–288. http://dx.doi.org/10.1126/science.289.5477.284.
Voutchkov, N., 2016. Desalination – Past, Present and Future. http://www.iwa-network.org/desalination-past-present-future/.
Wallis, P.J., Ward, M.B., Pittock, J., Hussey, K., Bamsey, H., Denis, A., Kenway, S.J., King, C.W., Mushtaq, S., Retamal, M.L., Spies, B.R., 2014. The water impacts of climate change mitigation measures. Clim. Change 125 (2), 209–220. http://dx.doi.org/10.1007/s10584-014-1156-6.
Wang, Y.Q., Lior, N., 2007a. Performance analysis of combined humidified gas turbine power generation and multi-effect thermal vapor compression desalination systems – Part 2: The evaporative gas turbine based system and some discussions. Desalination 207 (1–3), 243–256. http://dx.doi.org/10.1016/j.desal.2006.06.013.
Wang, Y.Q., Lior, N., 2007b. Fuel allocation in a combined steam-injected gas turbine and thermal seawater desalination system. Desalination 214 (1–3), 306–326. http://dx.doi.org/10.1016/j.desal.2007.01.001.
Wu, L., Hu, Y., Gao, C., 2013. Optimum design of cogeneration for power and desalination to satisfy the demand of water and power. Desalination 324, 111–117. http://dx.doi.org/10.1016/j.desal.2013.06.006.